
RCoT-Seg: Reinforced Chain-of-Thought for Video Reasoning and Segmentation

Junwei Wen^{1*} Deshui Miao^{1*} Guangming Lu¹ Xin Li^{1,2,3†} Wenjie Pei^{1,2†}

¹Harbin Institute of Technology, Shenzhen ²Pengcheng Laboratory

³Pazhou Lab (Huangpu)

Abstract

Video Reasoning Segmentation (VRS) aims to segment target objects in videos based on implicit instructions that convey human intent and temporal logic. Existing MLLM-based methods predict masks with a [SEG] token after selecting frames via simple sampling or an auxiliary MLLM, where limited supervision and frame-language similarity rules often yield narrow-scope keyframe choices that weaken holistic temporal understanding and lead to brittle localization in complex multi-object scenes. To address these issues, we introduce RCoT-Seg, a video-of-thought framework that factorizes VRS into temporal video reasoning (TVR) and keyframe target perception (KTP), explicitly separating temporal reasoning from spatial perception. Specifically, in the TVR stage, an agentic keyframe selection module, initialized with a curated CoT-start corpus and refined by GRPO under task-aligned rewards, is proposed to generate and reselect the keyframe through self-evaluation, strengthening moment localization and temporal reasoning. In the KTP stage, RCoT-Seg performs high-resolution segmentation on the selected frame and propagates masks with SAM2-based methods across the sequence, replacing heuristic sampling and external selectors while improving spatial precision and inter-frame consistency. Extensive experimental results demonstrate that the proposed RCoT-Seg achieves favorable performance against the state-of-the-art methods. The code and models will be publicly released at <https://github.com/Victor-wjw/RCoT-Seg>.

1 Introduction

Video reasoning segmentation (VRS) [30, 32] aims to generate pixel-level mask sequences from natural-language queries that involve commonsense grounding and implicit temporal logic, typically with multimodal large language models (MLLMs) [30, 3]. Despite recent progress, VRS remains challenging because the model must identify the temporally valid evidence implied by the query and further ground the target object with fine-grained spatial precision across diverse video scenarios.

Most existing methods [30, 8, 13] follow a “sample-then-segment” paradigm, where sparse frames are first obtained by uniform sampling, auxiliary MLLM filtering, or vision-language similarity-based screening, and then used for target localization and mask generation. However, such frame selection is usually treated as a one-shot pre-processing step rather than a verifiable decision. Once the selected frame fails to satisfy the language-conditioned temporal requirement, the downstream segmentation stage has limited ability to recover the missing evidence.

Recently, a concurrent work Veason-R1 [7] shows that CoT initialization and GRPO can improve VRS by encouraging reasoning before segmentation. Nevertheless, it still operates on a sparse sampled

*Equal contribution.

†Corresponding authors.

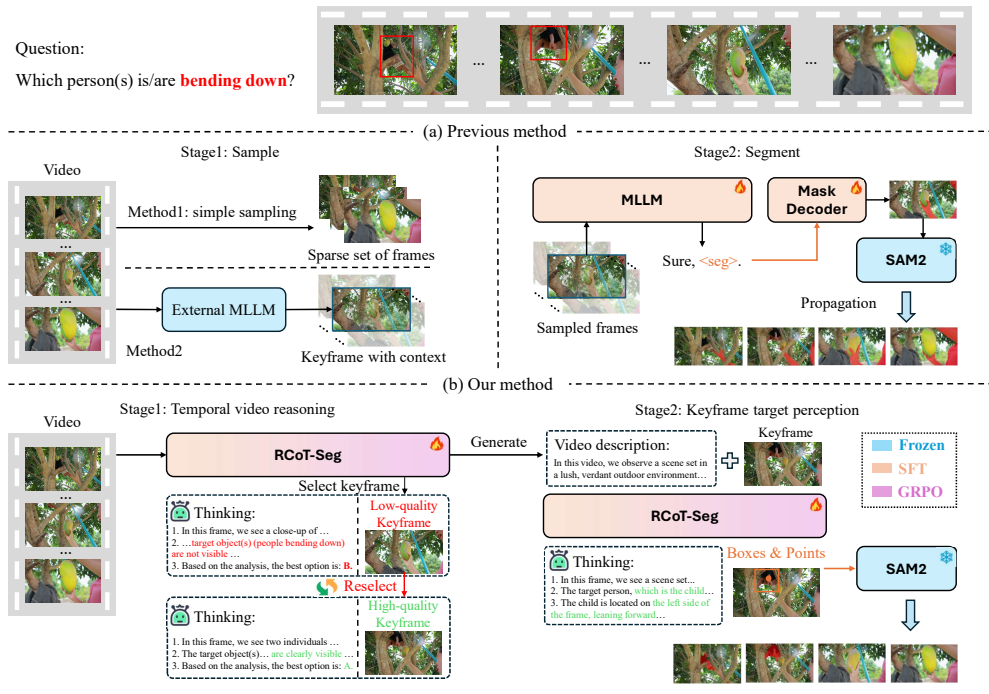


Figure 1: **Comparison between RCoT-Seg and previous methods.** RCoT-Seg segments the correct target through explicit CoT reasoning and concise keyframe selection.

view and commits to keyframe localization and spatial grounding within a single reasoning trajectory. As a result, keyframe reliability is not explicitly modeled as a controllable intermediate state, making it difficult to diagnose an unreliable keyframe or request an alternative temporal observation. To address these limitations, we propose **RCoT-Seg**, a reinforcement learning framework that treats VRS as an explicit chain-of-thought (CoT) process and decomposes it into two coupled sub-processes: *temporal video reasoning* (TVR) and *keyframe target perception* (KTP). RCoT-Seg resolves this tension by making CoT an *actionable intermediate state*—a semantic scaffold that is produced by TVR and consumed by KTP. Instead of relying on pre-sampling, the TVR stage scans the video to infer event structure and temporal conditions implied by the query, and selects a keyframe that best satisfies these conditions. The KTP stage then operates exclusively on this keyframe with high-resolution perception to produce accurate masks.

A central component of RCoT-Seg is an **agentic keyframe selection** mechanism with a lightweight self-critical loop. Beyond outputting a keyframe index, the selector learns to assess whether the current selection is *satisfied* or *unsatisfied* with respect to the query, and triggers *re-selection* when the evidence is insufficient. This self-evaluation capability turns keyframe selection from a one-shot heuristic into a verifiable decision process, substantially improving reliability under ambiguous temporal language, occlusion, and multi-object distractions. For segmentation, KTP conditions on both the selected keyframe and a compact video description generated in TVR, using this CoT-derived semantic scaffold to disambiguate targets and guide mask generation while retaining global context.

To enable structured multi-task reasoning, we curate a **28K-sample CoT dataset** to cold-start a base Qwen2.5-VL-3B model with supervised fine-tuning. Using customized prompt templates, Qwen2.5-VL-7B generates CoT reasoning traces for both agentic keyframe selection and keyframe target grounding. We then boost the model with GRPO-based reinforcement learning using task-specific datasets and rewards. In particular, for keyframe target grounding, we design a Hungarian algorithm-based reward to robustly handle multi-object scenarios and complex visual settings, providing stable credit assignment for accurate matching between predicted masks and target references. Extensive experiments demonstrate that RCoT-Seg achieves state-of-the-art performance across video reasoning segmentation and referring segmentation benchmarks.

Our contributions are summarized as follows:

- We propose **RCoT-Seg**, a reasoning-enhanced VRS framework that goes beyond single-pass reasoning by factorizing segmentation into *temporal video reasoning* and *keyframe target perception*. This design turns CoT from a passive explanation into an actionable intermediate state that bridges video-level temporal understanding and high-resolution mask generation.
- We develop **Agentic Keyframe Selection**, a self-checkable keyframe decision mechanism that explicitly judges whether the selected frame provides sufficient evidence for the query and triggers re-selection when necessary. This improves robustness over one-pass keyframe localization under implicit temporal instructions, occlusion, and multi-object distractions.
- We introduce a **matching-aware reward** (Hungarian-based) for RL refinement in keyframe grounding, and show strong empirical gains, achieving state-of-the-art results on multiple VRS and referring segmentation benchmarks.

2 Related work

2.1 Video reasoning segmentation

Video Reasoning Segmentation (VRS) is an emerging task that requires multimodal reasoning to segment target objects in videos based on natural language queries [3, 30, 32]. Pioneering works like VISA [30] combine an additional MLLM for keyframe sampling, followed by another MLLM for temporal reasoning and segmentation, and employ an object tracker for mask propagation. VideoLISA [3] introduces a sparse-to-dense sampling strategy and a One-Token-Seg-All paradigm, achieving video-level segmentation through a unified token representation. HyperSeg [25] generalizes the unified reasoning framework via a hybrid entity recognition mechanism, supporting cross-domain segmentation and enabling universal segmentation for both image and video inputs. Further advancements include GLUS [13], which provides MLLM with both global and local contexts that are further enhanced with end-to-end optimized VOS memory modules to improve the consistency, and VRS-HQ [8], which enhances temporal consistency through token fusion and utilizes SAM2 for occlusion-aware keyframe selection.

Token-based designs compress object information into a single token, which weakens alignment to the true referent with no explicit chain of thought. In addition, these methods either sample frames in ways that break temporal coherence or offload keyframe selection to auxiliary MLLMs, undermining end-to-end learning. Veason-R1 [7] still treats keyframe localization as a single-pass committed prediction. Once the selected keyframe is unreliable, the subsequent grounding stage has no explicit mechanism to detect the failure or request another temporal observation. Therefore, we design a comprehensive chain-of-thought reasoning pipeline and apply GRPO to improve its robustness, enabling explicit reasoning within a single model.

2.2 Visual fine-tuning via RL

Reinforcement learning [22] has become a significant paradigm for optimizing large language models, particularly demonstrating remarkable effectiveness in enhancing reasoning capabilities, as evidenced by ChatGPT-o1 [11]. Deepseek-R1 [9] introduces group relative policy optimization (GRPO), which leverages verifiable reward signals to estimate relative advantages among responses, thereby substantially improving reasoning. Building on this, GRPO fine-tuning techniques have been extended to multimodal tasks, covering areas such as image spatial reasoning [16, 23], video understanding [6, 12, 24], multi-image localization [2, 31], and visual generation [5, 28, 29], demonstrating its strong adaptability in complex multimodal scenarios. Early work, such as Seg-Zero [14] and VisionReasoner [15], designed task-specific rewards for segmentation, improving image-level reasoning and mask quality. Building on this idea, Omni-R1 [34] and Veason-R1 [7] adopted GRPO for Ref-AVS and VRS. Omni-R1 follows a cascaded dual-system design that depends on large training corpora and a strong pre-trained VRS backbone. Veason-R1 [7] further introduces CoT initialization and GRPO into VRS, demonstrating that reinforcement learning can improve keyframe localization and spatial grounding. Nevertheless, its inference process still produces keyframe localization and object grounding as a single committed reasoning trajectory, without explicitly modeling whether the selected keyframe is reliable enough for downstream segmentation. RCoT-Seg differs by making keyframe reliability an explicit decision state and introducing an agentic re-selection loop, thereby enabling the model to verify and revise temporal evidence before high-resolution target perception.

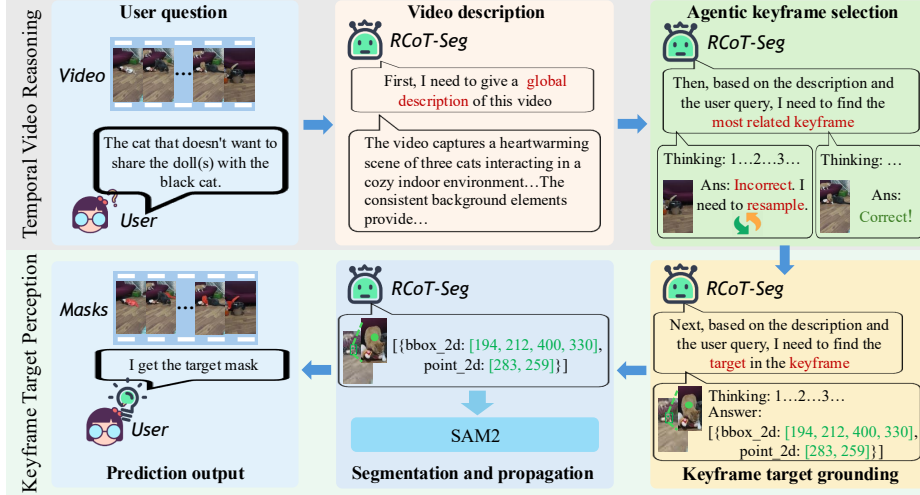


Figure 2: Overview of RCoT-Seg unified multi-task pipeline for VRS task.

In contrast, RCoT-Seg unifies temporal reasoning and segmentation in a single multi-task model, achieving stronger results in complex video scenarios with only modest training data.

3 Method

Given a video sequence and the query text of the target object(s), the goal of the proposed RCoT-Seg is to precisely localize the target object(s) with masks in each frame. To this end, the proposed RCoT-Seg first generates a video description as a compressed representation of the video content and selects a keyframe via agentic keyframe selection mechanism, then the object information of the target object(s) in the keyframe is obtained, which subsequently serves as prompts for the SAM2 [18] to perform mask generation and propagation, thereby achieving accurate segmentation of the target object(s).

3.1 Overview

Figure 2 illustrates the unified multi-task pipeline of our RCoT-Seg, consisting of two core stages: *Temporal Video Reasoning* and *Keyframe Target Perception*. Given a video sequence $\mathcal{V} \in \mathbb{R}^{T \times 3 \times H \times W}$ and an instruction text x_{ins} , RCoT-Seg first generates the video description x_{vid} , and the candidate keyframe z_{sel} which is evaluated and refined as final keyframe z_{key} via agentic keyframe selection mechanism. Then, RCoT-Seg predicts bounding boxes and points $\{(box_i, point_i)\}_{i=1}^{N_{obj}}$ of the target object(s) based on z_{key} and x_{vid} , which finally serves as prompts for the SAM2 to predict the segmentation masks $\mathcal{M} \in \mathbb{R}^{T \times H \times W}$.

As illustrated in Figure 3, we adopt a two-stage training paradigm. We initialize our framework with Qwen2.5-VL-3B [1] as the MLLM. In the first stage, we construct a hybrid chain-of-thought dataset and perform supervised fine-tuning. In the second stage, we apply GRPO [20, 9] to further enhance the capability in judging keyframe selection states and spatiotemporal localization of target objects.

3.2 Temporal video reasoning

Initial video reasoning. RCoT-Seg first exploits the inherent video reasoning capability of the foundation model via carefully designed prompts. Given a low-resolution, unsampled video sequence \mathcal{V} , our RCoT-Seg model φ_θ performs video description and keyframe generation:

$$x_{vid} = \varphi_\theta(\mathcal{V}, p_{vdg}), \quad z_{sel} = \varphi_\theta(\mathcal{V}, x_{ins}, p_{kfg}), \quad (1)$$

where p_{vdg} and p_{kfg} denote the prompts for video description and keyframe generation, respectively. The description x_{vid} acts as a compact representation of global semantics and the z_{sel} acts as the candidate keyframe.

Agentic keyframe selection (AKS). Although z_{sel} is obtained through the above reasoning, we empirically observe that the chosen keyframe can sometimes be suboptimal, and the one-step selection paradigm suffers from a lack of error tolerance. Therefore, an agentic mechanism is developed, which enables the model to autonomously evaluate and refine the chosen keyframe.

After the candidate keyframe is selected, RCoT-Seg decides whether the frame belongs to the valid keyframe set or its complement:

$$x_{\text{think}}^A, \text{ans} = \varphi_{\theta}(z_{sel}, x_{vid}, x_{ins}, p_{aks}), \quad \text{ans} \in \{A, B\}, \quad (2)$$

If $\text{ans} = A$, the frame is retained for segmentation (see Equation (5)); if $\text{ans} = B$, the model reselects a new keyframe by updating the prompt and invoking

$$z'_{sel} = \varphi_{\theta}(\mathcal{V}, x_{txt}, p'_{kfs}), \quad (3)$$

and the evaluation in Equation (2) is repeated until a satisfactory frame is obtained or a maximum iteration count λ is reached.

AKS GRPO reward. We use a two-component reward for AKS under GRPO, a format reward \mathcal{R}_f and an answer-accuracy reward \mathcal{R}_a . \mathcal{R}_f enforces structured outputs, which means the reasoning must appear inside `<think>...</think>` and the final decision inside `<answer>...</answer>`, and the decision must exactly match one of the prompt options. \mathcal{R}_a enforces answer correctness as:

$$\mathcal{R}_a = \begin{cases} 1.0, & \text{ans} = \text{ans}^{GT}, \\ 0.0, & \text{otherwise.} \end{cases} \quad (4)$$

where ans denotes the predicted option and ans^{GT} denotes the ground truth.

3.3 Keyframe target perception

Keyframe target grounding (KTG). RCoT-Seg receives a high-resolution keyframe z_{key} , the instruction x_{ins} , and the video description x_{vid} as context. Given a grounding prompt p_{ktg} , it outputs a thinking process and a list of cues:

$$x_{\text{think}}^G, \{(box_i, point_i)\}_{i=1}^{N_{obj}} = \varphi_{\theta}(z_{key}, x_{vid}, x_{ins}, p_{ktg}), \quad (5)$$

where $\{(box_i, point_i)\}_{i=1}^{N_{obj}}$ denotes the predicted bounding boxes and points for N_{obj} target objects in the keyframe, and x_{think}^G is the generated reasoning trace.

Keyframe segmentation and propagation. We then apply a frozen SAM2 model to segment each target and propagate masks across the video, using $(box_i, point_i)$ as prompts:

$$\mathcal{M}_i = \varphi_{\text{SAM2}}(z_{key}, (box_i, point_i), \mathcal{V}), \quad (6)$$

where φ_{SAM2} denotes SAM2 and \mathcal{V} is the video. The final prediction is obtained by aggregating per-object masks:

$$\mathcal{M} = \bigcup_{i=1}^{N_{obj}} \mathcal{M}_i. \quad (7)$$

KTG GRPO reward. To achieve KTG, the reward consists of a format reward \mathcal{R}_f and an answer accuracy reward \mathcal{R}_a . \mathcal{R}_f requires the same `<think> / <answer>` structure. The final answer must be a list of dictionaries with 2D boxes and points, such as `[{'bbox_2d': [x1, y1, x2, y2], 'point_2d': [x, y]}, ...]`. \mathcal{R}_a is designed to accommodate multi-object scenarios. Let the prediction be $\mathcal{P}_{BP} = \{(box_i, point_i)\}_{i=1}^{N_{obj}}$ and the ground truth $\mathcal{P}_{BP}^{GT} = \{(box_j^{GT}, point_j^{GT})\}_{j=1}^{N_{obj}^{GT}}$ on the resized 840×840 scale. Define binary score matrices (1=correct, 0=incorrect):

$$S_{i,j}^{\text{IoU}} = I_{\text{IoU} > \eta}(box_i, box_j^{GT}), \quad (8)$$

$$S_{i,j}^{\text{boxL1}} = I_{\text{L1} < \gamma_{\text{box}}}(box_i, box_j^{GT}), \quad (9)$$

$$S_{i,j}^{\text{ptL1}} = I_{\text{L1} < \gamma_{\text{pt}} \wedge \text{in-box}}(point_i, point_j^{GT}). \quad (10)$$

Aggregate them with weights $\alpha_{\text{IoU}}, \alpha_{\text{boxL1}}, \alpha_{\text{ptL1}}$:

$$S_{i,j} = \alpha_{\text{IoU}} S_{i,j}^{\text{IoU}} + \alpha_{\text{boxL1}} S_{i,j}^{\text{boxL1}} + \alpha_{\text{ptL1}} S_{i,j}^{\text{ptL1}}. \quad (11)$$

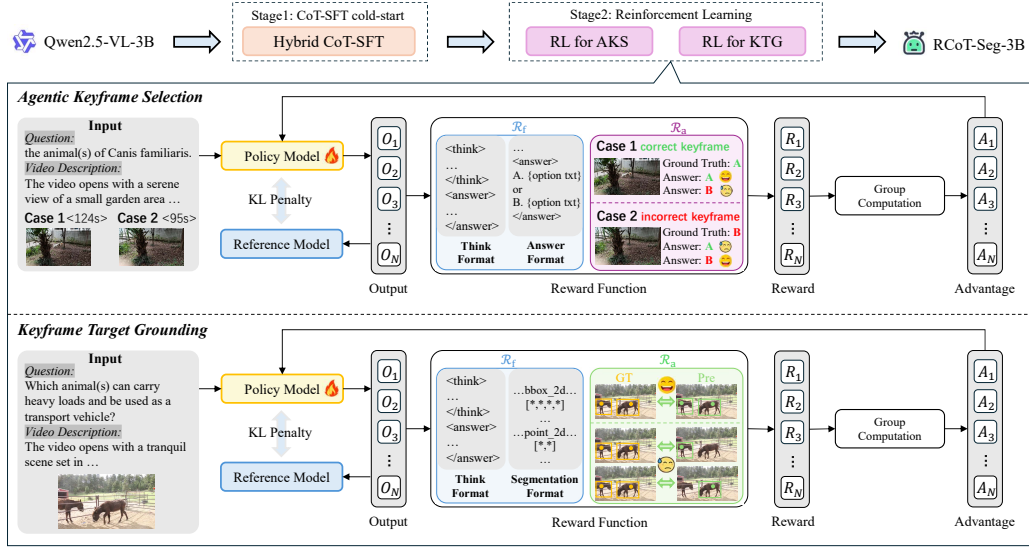


Figure 3: **Overall training strategy of RCoT-Seg.** Following a CoT-SFT cold-start, we employ GRPO reinforcement learning on the model using reward functions tailored to different tasks.

We obtain a one-to-one assignment by maximizing S with the Hungarian algorithm, yielding matched pairs C' . The answer accuracy reward averages the matched scores:

$$\mathcal{R}_a = \frac{1}{\max\{N_{\text{obj}}, N_{\text{obj}}^{GT}\}} \sum_{(i,j) \in C'} S_{i,j}. \quad (12)$$

3.4 Training strategy

Stage 1: CoT-SFT cold-start training. To stabilize reinforcement learning and avoid cold-start instability, we first construct a compact Chain-of-Thought dataset and perform cold-start supervised fine-tuning (CoT-SFT) on Qwen2.5-VL-3B, which serves as the initial RL actor.

We use Qwen2.5-VL-7B in a controlled data-generation pipeline to obtain step-wise reasoning traces. First, we define the keyframe as the frame whose annotated mask has the largest area. A structured CoT prompt guides the model to first analyze the scene, then describe the referred object(s), and finally localize them. Each instance is annotated with a bounding box and the center of its maximum inscribed circle. The prompt-annotation pair is then fed to Qwen2.5-VL-7B to produce the reasoning chain. For keyframe selection, we cast selection as a two-option decision: *Option A* is a valid keyframe instantiated as above, and *Option B* is sampled from frames with zero mask area. A fixed CoT prompt elicits reasoning chains, and we retain only those whose final option matches the ground truth.

Reasoning traces are wrapped in `<think> ...</think>` and final answers in `<answer> ...</answer>`. We sample from Ref-YouTube-VOS, MeViS, and ReVOS with a single-multi target ratio of 3:1 and an A-B ratio of 1:1, yielding **RCoT-Seg-SFT-28k**: 20k samples for KTG and 8k for AKS. To provide a stable initialization for subsequent GRPO training, we then jointly fine-tune Qwen2.5-VL-3B on RCoT-Seg-SFT-28k across both tasks using an autoregressive next-token objective with cross-entropy loss.

Stage 2: GRPO training. As illustrated in Figure 3, for each query q , the policy samples N responses $\{o_1, \dots, o_N\}$. Each response receives a verifiable, task-aligned reward \mathcal{R} , and we apply group-wise normalization to compute advantages (Eq. 14). Then, a KL penalty to a reference policy (the CoT-SFT model) stabilizes updates (Eq. 15).

We proportionally sample 4,000 and 6,000 instances different from those in SFT to construct the **RCoT-Seg-GRPO-AKS-4k** and **RCoT-Seg-GRPO-KTG-6k** datasets for AKS and KTG, respectively. For either task, the total reward is

$$\mathcal{R} = \lambda_f \mathcal{R}_f + \lambda_a \mathcal{R}_a, \quad (13)$$

Table 1: **Performance comparison on VRS datasets.** The best and second-best results are shown in **red** and **blue** color.

Method	Venue	ReVOS / referring			ReVOS / reasoning			ReVOS / overall			ReasonVOS		
		$\mathcal{J}\&\mathcal{F}$	\mathcal{J}	\mathcal{F}	$\mathcal{J}\&\mathcal{F}$	\mathcal{J}	\mathcal{F}	$\mathcal{J}\&\mathcal{F}$	\mathcal{J}	\mathcal{F}	$\mathcal{J}\&\mathcal{F}$	\mathcal{J}	\mathcal{F}
<i>Previous models using <seg> tokens for mask prediction via SFT training</i>													
VISA-7B [30]	ECCV2024	50.9	49.2	52.6	43.0	40.6	45.4	46.9	44.9	49.0	-	-	-
VISA-13B [30]	ECCV2024	57.4	55.6	59.1	44.3	42.0	46.7	50.9	48.8	52.9	-	-	-
VideoLISA-3.8B [3]	NeurIPS2024	-	-	-	-	-	-	-	-	-	47.5	45.1	49.9
InstructSeg-3B [26]	ICCV2025	57.0	54.8	59.2	51.9	49.2	54.7	54.5	52.0	56.9	-	-	-
HyperSeg-3B [25]	CVPR2025	58.5	56.0	60.9	53.0	50.2	55.8	55.7	53.1	58.4	-	-	-
GLUS-7B [13]	CVPR2025	58.3	56.0	60.7	51.4	48.8	53.9	54.8	52.4	57.3	49.9	47.5	52.4
VRS-HQ-7B [8]	CVPR2025	62.1	59.8	64.5	56.1	53.5	58.7	59.1	56.6	61.6	-	-	-
VRS-HQ-13B [8]	CVPR2025	63.3	61.1	65.5	56.8	54.1	59.4	60.0	57.6	62.5	-	-	-
<i>Latest models via GRPO training</i>													
Omni-R1-8B [34]	NeurIPS2025	61.6	-	-	50.7	-	-	56.2	-	-	-	-	-
Veason-R1-3B [7]	CVPR2026	63.0	60.3	65.6	56.8	53.6	60.0	59.9	56.9	62.8	55.2	51.8	58.5
RCoT-Seg-3B	-	64.3 (+1.0)	61.6	66.9	58.2 (+1.4)	54.9	61.6	61.2 (+1.2)	58.2	64.3	58.2 (+3.0)	54.6	61.8

and group-relative advantages are computed as

$$A_i = \frac{\mathcal{R}_i - \text{mean}(\{\mathcal{R}_1, \dots, \mathcal{R}_N\})}{\text{std}(\{\mathcal{R}_1, \dots, \mathcal{R}_N\})}. \quad (14)$$

The GRPO objective [20] is

$$\mathcal{J}_{\text{GRPO}}(\theta) = \mathbb{E}_{q, \{o_i\} \sim \pi_{\theta_{\text{old}}}} \left[\frac{1}{N} \sum_{i=1}^N \left(\min \left(\frac{\pi_{\theta}(o_i | q)}{\pi_{\theta_{\text{old}}}(o_i | q)} A_i, \right. \right. \right. \quad (15)$$

$$\left. \left. \left. \text{clip} \left(\frac{\pi_{\theta}(o_i | q)}{\pi_{\theta_{\text{old}}}(o_i | q)}, 1 - \epsilon, 1 + \epsilon \right) A_i \right) \right) - \beta \mathbb{D}_{\text{KL}}(\pi_{\theta} \| \pi_{\text{ref}}) \right]$$

where π_{ref} is the CoT-SFT model and β controls the KL strength.

4 Experiments

4.1 Datasets and metrics

Training datasets. We select training samples from the Ref-YouTube-VOS [19], MeViS [4], and ReVOS [30] training datasets according to a predefined ratio of single-multi and A-B. During the SFT stage, we adapt the Qwen2.5-VL-3B [1] model using the hybrid chain-of-thought dataset RCoT-Seg-SFT-28k, which is specifically designed for AKS and KTG tasks. In the GRPO training phase, we construct the RCoT-Seg-GRPO-AKS-4k and RCoT-Seg-GRPO-KTG-6k datasets for AKS and KTG, respectively.

Evaluation datasets. To comprehensively evaluate the performance of RCoT-Seg, we perform testing of RCoT-Seg across several benchmarks. These include two VRS datasets: ReVOS and ReasonVOS [3], as well as three RVOS datasets: DAVIS17 [17], Ref-YouTube-VOS, and MeViS [4].

Evaluation metrics. Following the evaluation in prior work [30], we employ three metrics: region similarity (\mathcal{J}), contour accuracy (\mathcal{F}), and their composite measure ($\mathcal{J}\&\mathcal{F}$). The \mathcal{J} metric computes the intersection-over-union (IoU) between the predicted mask sequence and the ground truth, while the \mathcal{F} metric assesses boundary alignment precision based on contour matching.

4.2 Implementation details

During the supervised fine-tuning (SFT) stage, we utilize the LLaMA-Factory framework [33] to fine-tune the Qwen2.5-VL-3B model with LoRA [10](rank=8) while freezing all other parameters. The training configuration employs a learning rate of 1×10^{-4} , cosine annealing scheduling, and 8-step gradient accumulation, conducting one training epoch on our chain-of-thought dataset RCoT-Seg-SFT-28k. In the reinforcement learning training phase, we implement the VERL framework [21] with a global batch size of 16, sampling 8 responses per input prompt to facilitate preference optimization. The model is trained for 500 and 1000 steps for AKS and KTG, respectively, using a learning rate of 1×10^{-6} . All experiments are conducted on 4 NVIDIA L20 GPUs.

Table 2: **Performance comparison on RVOS datasets.** The best and second-best results are shown in **red** and **blue** color.

Method	MLLM	DAVIS17			Ref-YouTube-VOS			MeViS		
		$\mathcal{J}\&\mathcal{F}$	\mathcal{J}	\mathcal{F}	$\mathcal{J}\&\mathcal{F}$	\mathcal{J}	\mathcal{F}	$\mathcal{J}\&\mathcal{F}$	\mathcal{J}	\mathcal{F}
Track-GPT-7B [35]	LLaVA-7B	63.2	59.4	67.0	56.4	55.3	57.4	40.1	37.6	42.6
Track-GPT-13B [35]	LLaVA-13B	66.5	62.7	70.4	59.5	58.1	60.8	41.2	39.2	43.1
VISA-7B [30]	Chat-UniVi-7B	69.4	66.3	72.5	61.5	59.8	63.2	43.5	40.7	46.3
VISA-13B [30]	Chat-UniVi-13B	70.4	67.0	73.8	63.0	61.4	64.7	44.5	41.8	47.1
VideoLISA-3.8B [3]	LLaVA-Phi-3-V	68.8	59.4	64.9	63.7	61.7	65.7	44.4	41.3	47.6
GLUS-7B [13]	LLaVA-7B	-	-	-	67.3	65.5	69.0	51.3	48.5	54.2
VRS-HQ-13B [8]	Chat-UniVi-13B	74.4	71.0	77.9	71.0	69.0	73.1	50.9	48.0	53.7
Veason-R1-3B [7]	Qwen2.5-VL-3B	-	-	-	-	-	-	51.2	48.2	54.2
RCoT-Seg(ours)	Qwen2.5-VL-3B	76.1 (+1.7)	72.2	80.0	72.5 (+1.5)	70.5	74.6	53.7 (+2.4)	50.7	56.7

4.3 Comparison results

Video reasoning segmentation. Table 1 presents a detailed performance comparison between RCoT-Seg and previous models [3, 30, 13, 8] trained via SFT using <seg> tokens for mask prediction, as well as the latest GRPO-trained model [34, 7]. Our method exhibits competitive performance compared to the leading state-of-the-art methods. Specifically, despite being fine-tuned on a limited number of samples, RCoT-Seg surpasses the previous SOTA model VRS-HQ-13B [8] by **1.2%** in $\mathcal{J}\&\mathcal{F}$ on ReVOS, and outperforms GLUS-7B [13] by **8.3%** in $\mathcal{J}\&\mathcal{F}$ on ReasonVOS, which stems primarily from the improved reasoning ability of our method. Furthermore, RCoT-Seg exceeds Omni-R1 [34] by approximately **5.0%** on ReVOS, demonstrating the incorporation of multi-task reasoning to guide precise segmentation. Moreover, RCoT-Seg achieves higher performance than the GRPO-based method, Veason-R1 [7], on both ReVOS (**+1.3%**) and ReasonVOS datasets (**+3.0%**), which underscores the efficacy of the agentic keyframe selection mechanism.

Table 3: Ablation on the proposed components. VDG, KFG and AKS denote Video Description Generation, Keyframe Generation, and Agentic Keyframe Selection, respectively. When KFG is not used, we select the first frame as the keyframe.

	VDG	KFG	AKS	Ref-YT-VOS	MeViS	ReVOS	ReasonVOS
				68.9	48.9	57.1	53.9
✓				69.1	49.8	57.7	54.9
	✓			70.5	51.7	59.5	54.4
		✓		70.8	52.2	60.3	55.7
✓	✓	✓		72.5	53.7	61.2	58.2

Table 5: Ablation on different training strategies. SFT^A denotes performing SFT on the agentic keyframe selection task, SFT^G denotes performing SFT on the keyframe target grounding task, and $SFT^{A,G}$ denotes performing SFT on both tasks.

Training Strategy	Referring			Reasoning		
	$\mathcal{J}\&\mathcal{F}$	\mathcal{J}	\mathcal{F}	$\mathcal{J}\&\mathcal{F}$	\mathcal{J}	\mathcal{F}
Qwen2.5-VL-3B	14.7	11.3	18.2	13.7	10.5	17.0
$SFT^{A,G}$	59.1	56.4	61.8	51.1	48.0	54.1
$GRPO^{A,G}$	62.8	60.1	65.5	55.5	52.3	58.8
$SFT^{A,G} + GRPO^G$	63.8	60.8	66.8	56.3	53.1	59.5
$SFT^G + GRPO^{A,G}$	63.0	60.3	65.6	57.0	54.0	60.0
$SFT^{A,G} + GRPO^{A,G}$	64.3	61.6	66.9	58.2	54.9	61.6

Referring VOS. Table 2 presents a performance comparison between RCoT-Seg and state-of-the-art RVOS methods across three benchmark datasets. The proposed RCoT-Seg surpasses VRS-HQ-13B [8] by **1.7%** in $\mathcal{J}\&\mathcal{F}$ on DAVIS17 and by **1.5%** in $\mathcal{J}\&\mathcal{F}$ on Ref-YouTube-VOS, while utilizing fewer parameters. On the more complex MeViS dataset, RCoT-Seg outperforms GLUS-7B [13] by **2.4%** in $\mathcal{J}\&\mathcal{F}$, highlighting the effectiveness in handling complex scenarios. Furthermore, RCoT-Seg

Table 4: Ablation on the maximum iteration count λ for agentic keyframe selection. $\lambda = 0$ indicates that AKS is not used. $\lambda = 5$ achieves the best performance, we select $\lambda = 5$ in default.

λ	DAVIS17	Ref-YT-VOS	MeViS	ReVOS	ReasonVOS
0	74.1	70.8	52.2	60.3	55.7
2	74.6	71.6	53.2	60.8	57.2
3	75.3	72.2	53.6	60.9	57.8
5	76.1	72.5	53.7	61.2	58.2
7	76.0	72.5	53.8	61.2	58.1
10	76.1	72.4	53.7	61.2	58.2

Table 6: Ablation on architecture. The separated architecture means we adopt CoT-SFT cold-start GRPO to train two separated models for completing the AKS and VTG tasks, while utilizing Qwen2.5-VL-3B to handle the VDG and KFG tasks. The unified architecture refers to the proposed RCoT-Seg.

Architecture	Referring			Reasoning		
	$\mathcal{J}\&\mathcal{F}$	\mathcal{J}	\mathcal{F}	$\mathcal{J}\&\mathcal{F}$	\mathcal{J}	\mathcal{F}
Separated	62.5	59.6	65.4	55.6	52.1	59.1
Unified	64.3	61.6	66.9	58.2	54.9	61.6

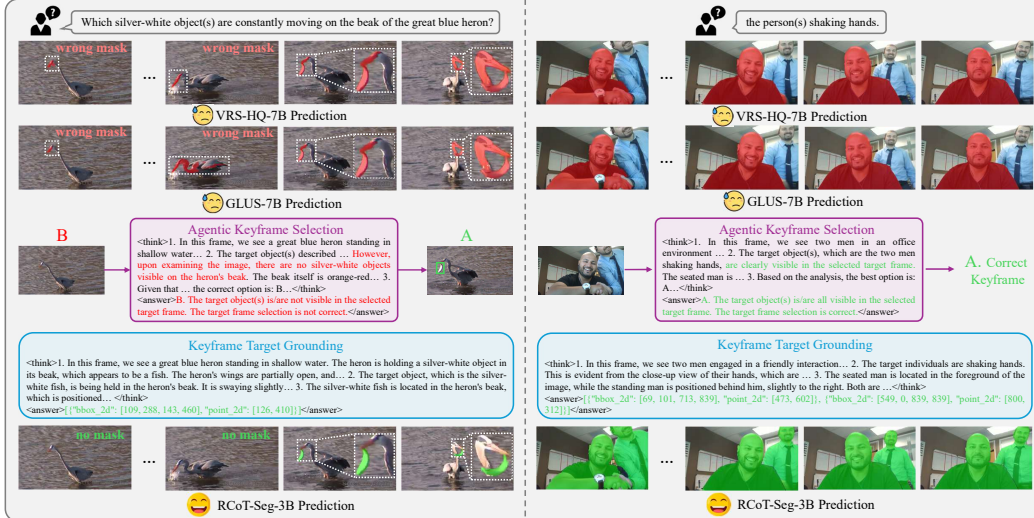


Figure 4: **Qualitative comparison between RCoT-Seg and current SOTA methods.** Our method successfully identify and accurately segment targets in complex scenarios involving small-scale objects and multi-object interactions.

exceeds Veason-R1 [7] by **2.5%** on the MeViS dataset, indicating the efficacy of the agentic keyframe selection mechanism.

4.4 Ablation Studies

Effect of the proposed components. As shown in Table 3, the adoption of our Video Description Generation, Keyframe Generation, and Agentic Keyframe Selection modules leads to substantial improvements (**+3.6** on Ref-YouTube-VOS, **+4.8** on MeViS, **+4.1** on ReVOS, **+4.3** on ReasonVOS).

Ablation on the maximum iteration count for AKS. Table 4 shows the impact of the maximum iteration count λ for AKS on the performance. The results indicate that a count of 5 achieves a favorable balance, yielding strong performance while reducing redundancy. Consequently, a threshold of 5 is adopted for our model during inference. We also analyze the inference time of this component. Please see Appendix C for details.

Effect of our training strategy. The results in Table 5 validates the efficacy of our training strategy. When SFT and GRPO are applied individually to the two tasks, the performance on ReVOS decreases by **5.2%** and **1.5%** in $\mathcal{J}\&\mathcal{F}$ on the referring subset, and by **7.1%** and **2.7%** in $\mathcal{J}\&\mathcal{F}$ on the reasoning subset, respectively. Furthermore, when GRPO and SFT are omitted individually for the AKS task, the performance on ReVOS decreases by **0.5%** and **1.3%** in $\mathcal{J}\&\mathcal{F}$ on the referring subset, and by **1.9%** and **1.2%** in $\mathcal{J}\&\mathcal{F}$ on the reasoning subset, respectively. This demonstrates the effectiveness of our multi-task, multi-stage training strategy.

Effect of our unified model. We attempt to address VRS under the separated architecture, which allocates different tasks to separated models. The results in Table 6 indicate that this separated architecture underperforms the proposed unified RCoT-Seg model by **1.8%** in $\mathcal{J}\&\mathcal{F}$ on the referring subset and by **2.6%** in $\mathcal{J}\&\mathcal{F}$ on the reasoning subset, demonstrating the efficacy of our unified architecture.

4.5 Qualitative comparison

Figure 4 qualitatively compares RCoT-Seg with VRS-HQ-7B [8] and GLUS-7B [13] in complex scenarios. For the left example, where the target object is small and appears only in a subset of frames, RCoT-Seg employs AKS to reselect the correct keyframe, thereby achieving a better segmentation result. In the right case, it is a multi-object scenario (two people shaking hands). Both VRS-HQ-7B [8] and GLUS-7B [13] segment only one of them, whereas our RCoT-Seg successfully segments all target objects.

5 Conclusion

In this work, we present RCoT-Seg, a unified model that accomplishes VRS through a sequential pipeline of temporal video reasoning and keyframe target perception trained with reinforcement learning. Unlike sampling-based paradigms, we propose an agentic keyframe selection to improve keyframe quality with a simple self-evolution mechanism. The KTP stage operates on the selected keyframe guided by a compact video description, which transfers long-horizon context to pixel-level decoding. To handle multi-object scenarios, we design a Hungarian-based matching reward that stabilizes training and strengthens object-wise consistency. The model is cold-started with the proposed hybrid CoT supervision and then optimized across tasks using GRPO, aligning reasoning traces with downstream segmentation behavior. Extensive experiments on standard benchmarks show that RCoT-Seg achieves state-of-the-art performance in video reasoning segmentation and video referring segmentation, validating the effectiveness of the global-to-local design, the agentic selection mechanism, and the explicit Chain-of-Thought guidance in VRS.

References

- [1] Shuai Bai, Keqin Chen, Xuejing Liu, Jialin Wang, Wenbin Ge, Sibao Song, Kai Dang, Peng Wang, Shijie Wang, Jun Tang, et al. Qwen2. 5-vl technical report. *arXiv preprint arXiv:2502.13923*, 2025.
- [2] Sule Bai, Mingxing Li, Yong Liu, Jing Tang, Haoji Zhang, Lei Sun, Xiangxiang Chu, and Yansong Tang. Univg-r1: Reasoning guided universal visual grounding with reinforcement learning. *arXiv preprint arXiv:2505.14231*, 2025.
- [3] Zechen Bai, Tong He, Haiyang Mei, Pichao Wang, Ziteng Gao, Joya Chen, Lei Liu, Zheng Zhang, and Mike Z Shou. One token to seg them all: Language instructed reasoning segmentation in videos. *Advances in Neural Information Processing Systems*, 37:6833–6859, 2024.
- [4] Henghui Ding, Chang Liu, Shuting He, Xudong Jiang, and Chen Change Loy. Mevis: A large-scale benchmark for video segmentation with motion expressions. In *Proceedings of the IEEE/CVF international conference on computer vision*, pages 2694–2703, 2023.
- [5] Rongyao Fang, Chengqi Duan, Kun Wang, Linjiang Huang, Hao Li, Shilin Yan, Hao Tian, Xingyu Zeng, Rui Zhao, Jifeng Dai, et al. Got: Unleashing reasoning capability of multimodal large language model for visual generation and editing. *arXiv preprint arXiv:2503.10639*, 2025.
- [6] Kaituo Feng, Kaixiong Gong, Bohao Li, Zonghao Guo, Yibing Wang, Tianshuo Peng, Junfei Wu, Xiaoying Zhang, Benyou Wang, and Xiangyu Yue. Video-r1: Reinforcing video reasoning in mllms. *arXiv preprint arXiv:2503.21776*, 2025.
- [7] Sitong Gong, Lu Zhang, Yunzhi Zhuge, Xu Jia, Pingping Zhang, and Huchuan Lu. Reinforcing video reasoning segmentation to think before it segments. *arXiv preprint arXiv:2508.11538*, 2025.
- [8] Sitong Gong, Yunzhi Zhuge, Lu Zhang, Zongxin Yang, Pingping Zhang, and Huchuan Lu. The devil is in temporal token: High quality video reasoning segmentation. In *Proceedings of the Computer Vision and Pattern Recognition Conference*, pages 29183–29192, 2025.
- [9] Daya Guo, Dejian Yang, Haowei Zhang, Junxiao Song, Ruoyu Zhang, Runxin Xu, Qihao Zhu, Shirong Ma, Peiyi Wang, Xiao Bi, et al. Deepseek-r1: Incentivizing reasoning capability in llms via reinforcement learning. *arXiv preprint arXiv:2501.12948*, 2025.
- [10] Edward J Hu, Yelong Shen, Phillip Wallis, Zeyuan Allen-Zhu, Yuanzhi Li, Shean Wang, Lu Wang, Weizhu Chen, et al. Lora: Low-rank adaptation of large language models. *ICLR*, 1(2):3, 2022.
- [11] Aaron Jaech, Adam Kalai, Adam Lerer, Adam Richardson, Ahmed El-Kishky, Aiden Low, Alec Helyar, Aleksander Madry, Alex Beutel, Alex Carney, et al. Openai o1 system card. *arXiv preprint arXiv:2412.16720*, 2024.

- [12] Xinhao Li, Ziang Yan, Desen Meng, Lu Dong, Xiangyu Zeng, Yinan He, Yali Wang, Yu Qiao, Yi Wang, and Limin Wang. Videochat-r1: Enhancing spatio-temporal perception via reinforcement fine-tuning. *arXiv preprint arXiv:2504.06958*, 2025.
- [13] Lang Lin, Xueyang Yu, Ziqi Pang, and Yu-Xiong Wang. Glus: Global-local reasoning unified into a single large language model for video segmentation. In *Proceedings of the Computer Vision and Pattern Recognition Conference*, pages 8658–8667, 2025.
- [14] Yuqi Liu, Bohao Peng, Zhisheng Zhong, Zihao Yue, Fanbin Lu, Bei Yu, and Jiaya Jia. Seg-zero: Reasoning-chain guided segmentation via cognitive reinforcement. *arXiv preprint arXiv:2503.06520*, 2025.
- [15] Yuqi Liu, Tianyuan Qu, Zhisheng Zhong, Bohao Peng, Shu Liu, Bei Yu, and Jiaya Jia. Vision-reasoner: Unified visual perception and reasoning via reinforcement learning. *arXiv preprint arXiv:2505.12081*, 2025.
- [16] Ziyu Liu, Zeyi Sun, Yuhang Zang, Xiaoyi Dong, Yuhang Cao, Haodong Duan, Dahua Lin, and Jiaqi Wang. Visual-rft: Visual reinforcement fine-tuning. *arXiv preprint arXiv:2503.01785*, 2025.
- [17] Jordi Pont-Tuset, Federico Perazzi, Sergi Caelles, Pablo Arbeláez, Alex Sorkine-Hornung, and Luc Van Gool. The 2017 davis challenge on video object segmentation. *arXiv preprint arXiv:1704.00675*, 2017.
- [18] Nikhila Ravi, Valentin Gabeur, Yuan-Ting Hu, Ronghang Hu, Chaitanya Ryali, Tengyu Ma, Haitham Khedr, Roman Rädle, Chloe Rolland, Laura Gustafson, et al. Sam 2: Segment anything in images and videos. *arXiv preprint arXiv:2408.00714*, 2024.
- [19] Seonguk Seo, Joon-Young Lee, and Bohyung Han. Urvos: Unified referring video object segmentation network with a large-scale benchmark. In *Computer Vision—ECCV 2020: 16th European Conference, Glasgow, UK, August 23–28, 2020, Proceedings, Part XV 16*, pages 208–223. Springer, 2020.
- [20] Zhihong Shao, Peiyi Wang, Qihao Zhu, Runxin Xu, Junxiao Song, Xiao Bi, Haowei Zhang, Mingchuan Zhang, YK Li, Yang Wu, et al. Deepseekmath: Pushing the limits of mathematical reasoning in open language models. *arXiv preprint arXiv:2402.03300*, 2024.
- [21] Guangming Sheng, Chi Zhang, Zilingfeng Ye, Xibin Wu, Wang Zhang, Ru Zhang, Yanghua Peng, Haibin Lin, and Chuan Wu. Hybridflow: A flexible and efficient rlhf framework. In *Proceedings of the Twentieth European Conference on Computer Systems*, pages 1279–1297, 2025.
- [22] Richard S Sutton, Andrew G Barto, et al. *Reinforcement learning: An introduction*, volume 1. MIT press Cambridge, 1998.
- [23] Song Wang, Gongfan Fang, Lingdong Kong, Xiangtai Li, Jianyun Xu, Sheng Yang, Qiang Li, Jianke Zhu, and Xinchao Wang. Pixelthink: Towards efficient chain-of-pixel reasoning. *arXiv preprint arXiv:2505.23727*, 2025.
- [24] Ye Wang, Ziheng Wang, Boshen Xu, Yang Du, Kejun Lin, Zihan Xiao, Zihao Yue, Jianzhong Ju, Liang Zhang, Dingyi Yang, et al. Time-r1: Post-training large vision language model for temporal video grounding. *arXiv preprint arXiv:2503.13377*, 2025.
- [25] Cong Wei, Yujie Zhong, Haoxian Tan, Yong Liu, Zheng Zhao, Jie Hu, and Yujiu Yang. Hyperseg: Towards universal visual segmentation with large language model. *arXiv preprint arXiv:2411.17606*, 2024.
- [26] Cong Wei, Yujie Zhong, Haoxian Tan, Yingsen Zeng, Yong Liu, Hongfa Wang, and Yujiu Yang. Instructseg: Unifying instructed visual segmentation with multi-modal large language models. In *Proceedings of the IEEE/CVF International Conference on Computer Vision*, pages 20193–20203, 2025.

- [27] Zhuofan Xia, Dongchen Han, Yizeng Han, Xuran Pan, Shiji Song, and Gao Huang. Gsva: Generalized segmentation via multimodal large language models. In *Proceedings of the IEEE/CVF Conference on Computer Vision and Pattern Recognition*, pages 3858–3869, 2024.
- [28] Yicheng Xiao, Lin Song, Yukang Chen, Yingmin Luo, Yuxin Chen, Yukang Gan, Wei Huang, Xiu Li, Xiaojuan Qi, and Ying Shan. Mindomni: Unleashing reasoning generation in vision language models with rgpo. *arXiv preprint arXiv:2505.13031*, 2025.
- [29] Zeyue Xue, Jie Wu, Yu Gao, Fangyuan Kong, Lingting Zhu, Mengzhao Chen, Zhiheng Liu, Wei Liu, Qiushan Guo, Weilin Huang, et al. Dancegrp: Unleashing grp on visual generation. *arXiv preprint arXiv:2505.07818*, 2025.
- [30] Cilin Yan, Haochen Wang, Shilin Yan, Xiaolong Jiang, Yao Hu, Guoliang Kang, Weidi Xie, and Efstratios Gavves. Visa: Reasoning video object segmentation via large language models. In *European Conference on Computer Vision*, pages 98–115. Springer, 2024.
- [31] Bob Zhang, Haoran Li, Tao Zhang, Cilin Yan, Jiayin Cai, and Yanbin Hao. Improving the reasoning of multi-image grounding in mllms via reinforcement learning. *arXiv preprint arXiv:2507.00748*, 2025.
- [32] Rongkun Zheng, Lu Qi, Xi Chen, Yi Wang, Kun Wang, Yu Qiao, and Hengshuang Zhao. Villa: Video reasoning segmentation with large language model. *arXiv preprint arXiv:2407.14500*, 2024.
- [33] Yaowei Zheng, Richong Zhang, Junhao Zhang, Yanhan Ye, Zheyang Luo, Zhangchi Feng, and Yongqiang Ma. Llamafactory: Unified efficient fine-tuning of 100+ language models. *arXiv preprint arXiv:2403.13372*, 2024.
- [34] Hao Zhong, Muzhi Zhu, Zongze Du, Zheng Huang, Canyu Zhao, Mingyu Liu, Wen Wang, Hao Chen, and Chunhua Shen. Omni-r1: Reinforcement learning for omnimodal reasoning via two-system collaboration. *arXiv preprint arXiv:2505.20256*, 2025.
- [35] Jiawen Zhu, Zhi-Qi Cheng, Jun-Yan He, Chenyang Li, Bin Luo, Huchuan Lu, Yifeng Geng, and Xuansong Xie. Tracking with human-intent reasoning. *arXiv preprint arXiv:2312.17448*, 2023.

Prompt for Qwen2.5-VL-7B to generate CoT for AKS task

<image> The above is a target frame selected from a video, and the text description of the video is: "{Video_Description}"
 The text description of the target object(s) is: "{Question}"
 Please determine which of the following two options best describes the state of the target object(s) in the selected target frame:
 A. The target object(s) is/are all visible in the selected target frame. The target frame selection is correct.
 B. The target object(s) is/are not visible in the selected target frame. The target frame selection is not correct.
 You need to follow the steps below to reason step-by-step naturally:
 1. Briefly describe what is happening in this frame.
 2. Determine whether the target object(s) is/are visible in the selected target frame.
 3. Select the best option.

Prompt for Qwen2.5-VL-7B to generate CoT for KTG task

<image> The above is a frame from a video, and the text description of the video is: "{Video_Description}". One or more objects are marked with red rectangles in each frame.
 The text description of the target object(s) is: "{Question}"
 You must base your reasoning on this frame. Please follow this reasoning process step-by-step:
 1. Briefly describe what is happening in this frame.
 2. Describe what the target(s) is/are doing.
 3. Detect Precisely where it/they is/are located in this frame.
 Important: - Do not refer to or describe the red rectangles.
 - Write naturally, but follow the reasoning steps clearly.

Figure 5: Prompt templates for CoT datasets generation.

Prompt for Video Description Generation

<video> Please provide a descriptive text based on the input video. The description should cover all objects in the video, as well as the state changes of different elements if they exist. Additionally, it should include the relationships between different objects and their behavioral logic if applicable. The description should be as detailed as possible within 1000 words.

Figure 6: Prompt templates for VDG task.

A More implement details

A.1 Datasets construction

Figure 5 illustrates the prompt templates for Qwen2.5-VL-7B [1] to generate Chain-of-Thought data. Each prompt is presented to the model along with a selected keyframe (resized to 840×840) and its corresponding video description, as well as the predefined description of the target object(s). The methods for selecting keyframes for both tasks have been discussed in the main document. The corresponding video descriptions are generated by our base model Qwen2.5-VL-3B [1] prompted by Figure 6 and incorporated into our RCoT-Seg-SFT-28k, RCoT-Seg-GRPO-AKS-4k and RCoT-Seg-GRPO-KTG-6k datasets. The prompts guide the model to (i) briefly describe the scene, (ii) analyze the target object(s), and (iii) complete the task. For each piece of generated CoT data, we select those that meet our task requirements and discard the lower-quality ones. The composition of the training datasets and several sample examples are shown in Figure 7.

A.2 Training settings

The training process of our model is divided into two main stages: CoT-SFT and GRPO, and the details of our training approach are shown in Table 7. In the first stage, we construct a compact Chain-of-Thought dataset RCoT-Seg-SFT-28k, and perform cold-start supervised fine-tuning (CoT-SFT) on Qwen2.5-VL-3B [1] with LoRA [10] to mitigate overfitting. In the second stage, we use GRPO [20, 9] for reinforcement learning refinement with 4K and 6K task-specific datasets, respectively. The training is conducted on 4 NVIDIA L20 GPUs, which takes about 3 days to finish the whole multi-stage training.

During GRPO training, we design a task-aligned verifiable reward \mathcal{R} to optimize model behavior, which is obtained by adding the format reward \mathcal{R}_f and the answer accuracy reward \mathcal{R}_a with corresponding weights λ_f and λ_a . For the AKS task, λ_f and λ_a are set to 1.0 and 2.0, respectively. The format reward checks the overall format of the output, with a full score of 1.0. The accuracy reward checks the correctness of the predicted answer, with a full score of 1.0. Therefore, the maximum total reward for the AKS task is 3.0. For the KTG task, λ_f and λ_a are set to 1.0 and 1.0, respectively.

Table 7: Training parameters.

Config	CoT-SFT	AKS-GRPO	KTG-GRPO
finetuning type	LoRA	GRPO	GRPO
optimizer	AdamW	AdamW	AdamW
learning rate	1e-4	1e-6	1e-6
weight decay	0.0	0.01	0.01
batch size	8	16	16
lora rank	8	-	-
gradient-accumulation-steps	8	-	-
lr scheduler	cosine	constant	constant
warmup ratio	0.1	0.0	0.0
kl loss coef	-	0.01	0.01
kl loss type	-	low-var-kl	low-var-kl
rollout-n	1	8	8
temperature	0.95	1.0	1.0
top-k	50	-1	-1
top-p	0.7	1.0	1.0
max prompt length	3000	3000	3000
max response length	1024	2000	2000
training epochs	1	-	-
training steps	-	500	1000
training set	RCoT-Seg-SFT-28k	RCoT-Seg-GRPO-AKS-4k	RCoT-Seg-GRPO-KTG-6k

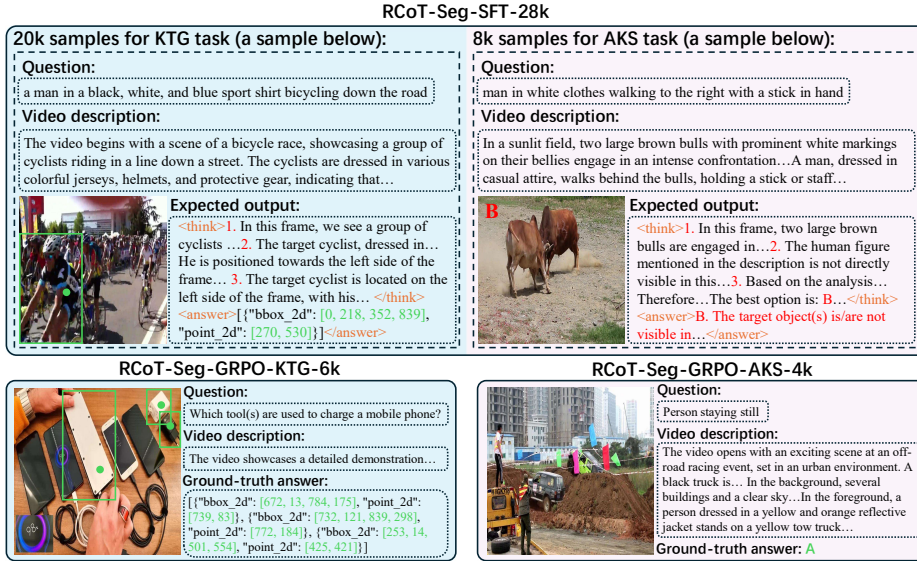


Figure 7: Composition of the training datasets and sample examples.

The format reward further examines the format of the predicted bounding boxes and points, with a maximum score of 3.0. The accuracy reward evaluates the IoU metric and L1 distance between predicted bounding boxes and the ground truth, as well as the L1 distance between predicted points and the ground truth, with a maximum score of 3.0. The threshold hyperparameters η , γ_{box} , and γ_{pt} are set to 0.5, 10, and 30, respectively. The maximum total reward for the KTG task is 6.0.

A.3 Inference details

The prompt templates used for Video Description Generation and Keyframe Generation are shown in Figure 6 and Figure 9, respectively. Additionally, the prompt templates used for AKS and KTG tasks are shown in Figure 8. During Video Description Generation and Keyframe Generation, the proposed RCoT-Seg receives the full video sequence, where each frame is resized to 448×448 . In contrast, when performing AKS and KTG tasks, the input keyframe is resized to 840×840 to enhance detail perception.

Prompt for AKS task

<image> The above is a target frame selected from a video, and the text description of the video is: "{Video_Description}"
 The text description of the target object(s) is: "{Question}"
 Please determine which of the following two options best describes the state of the target object(s) in the selected target frame:
 A. The target object(s) is/are all visible in the selected target frame. The target frame selection is correct.
 B. The target object(s) is/are not visible in the selected target frame. The target frame selection is not correct.
 You need to follow the steps below to output your thinking process step-by-step naturally:
 1. Briefly describe what is happening in this frame.
 2. Determine whether the target object(s) is/are visible in the selected target frame.
 3. Select the best option.
 Output the thinking process in <think> </think> and final answer in <answer> </answer> tags.
 i.e., <think> thinking process here </think>
 <answer>A. The target object(s) is/are all visible in the selected target frame. The target frame selection is correct.</answer>

Prompt for KTG task

<image> The above is a frame from a video, and the text description of the video is: "{Video_Description}"
 Please find "{Question}" with bboxes and points.
 You should first output your thinking process, then provide the final answer. You must base your reasoning on this frame.
 Your thinking process should follow this reasoning process step-by-step:
 1. Briefly describe what is happening in this frame.
 2. Describe what the target(s) is/are doing.
 3. Detect Precisely where it/they is/are located in this frame.
 Output the thinking process in <think> </think> and final answer in <answer> </answer> tags.
 Output the bbox(es) and point(s) inside the interested object(s) in JSON format.
 i.e., <think> thinking process here </think>\n<answer>[{"bbox_2d": [378,494,546,796], "point_2d": [518,551]}, {"bbox_2d": [507,272,647,647], "point_2d": [643,388]}]</answer>

Figure 8: Prompt templates for AKS and KTG tasks.

Prompt for Keyframe Generation

<0s><image>, <1s><image>, <191s><image>, <192s><image>
 You are given a 1FPS video which has {Num} frames. Each image is preceded by its timestamp. Given the object(s) description: "{Question}", please select a key frame from the video that reasonably matches the description. Output the timestamp of the key frame. i.e., keyframe-timestamp: <your answer> (e.g., keyframe-timestamp: <0s>).
 Important: - We already know that frame(s) at {Timestamp_List} is/are incorrect, and your answer timestamp should be different. Only for keyframe reselection

Figure 9: Prompt templates for KFG task.

B Effect of scaling model size

To investigate the impact of foundation model capacity on our framework, we train a larger variant initialized from Qwen2.5-VL-7B. This model follows the exact same multi-stage training pipeline (CoT-SFT and GRPO) and hyperparameters as the 3B variant. Notably, the training datasets remain identical to those used for RCoT-Seg-3B. The video descriptions are still generated by the 3B model, and the CoT reasoning traces continue to be constructed using the 7B model.

As detailed in Table 8 and Table 9, scaling the model size yields consistent improvements across VRS and RVOS benchmarks.

C Timing analysis

We analyze the additional time consumption required to complete VDG, KFG, and AKS tasks compared to performing only the KTG task. We set the time consumption for the KTG task as 1.0, which includes the time taken by SAM2 [18] for keyframe segmentation and propagation. As shown in Figure 10, completing the VDG, KFG, and AKS tasks requires additional time consumption of 0.21, 0.60, and 1.47 respectively. Without using AKS, the inference time consumption is 1.81. The additional time consumption incurred by adopting AKS is 1.47. Therefore, implementing the AKS mechanism results in an 81% increase in additional time consumption.

Our evaluation reveals that the latency overhead primarily stems from repeated full-video encoding during the AKS re-evaluation phase, rather than from the AKS mechanism itself. To verify this and optimize efficiency, we introduce a light re-evaluation strategy: while maintaining the initial encoding pass on the full video, we replace subsequent re-evaluations with 16 uniformly sampled frames. As

Table 8: **Performance comparison on VRS datasets.** The best and second-best results are shown in **red** and **blue** color.

Method	ReVOS / referring			ReVOS / reasoning			ReVOS / overall			ReasonVOS		
	$\mathcal{J}\&\mathcal{F}$	\mathcal{J}	\mathcal{F}	$\mathcal{J}\&\mathcal{F}$	\mathcal{J}	\mathcal{F}	$\mathcal{J}\&\mathcal{F}$	\mathcal{J}	\mathcal{F}	$\mathcal{J}\&\mathcal{F}$	\mathcal{J}	\mathcal{F}
<i>Previous models using <seg> tokens for mask prediction via SFT training</i>												
VISA-7B [30]	50.9	49.2	52.6	43.0	40.6	45.4	46.9	44.9	49.0	-	-	-
VISA-13B [30]	57.4	55.6	59.1	44.3	42.0	46.7	50.9	48.8	52.9	-	-	-
VideoLISA-3.8B [3]	-	-	-	-	-	-	-	-	-	47.5	45.1	49.9
InstructSeg-3B [26]	57.0	54.8	59.2	51.9	49.2	54.7	54.5	52.0	56.9	-	-	-
HyperSeg-3B [25]	58.5	56.0	60.9	53.0	50.2	55.8	55.7	53.1	58.4	-	-	-
GLUS-7B [13]	58.3	56.0	60.7	51.4	48.8	53.9	54.8	52.4	57.3	49.9	47.5	52.4
VRS-HQ-7B [8]	62.1	59.8	64.5	56.1	53.5	58.7	59.1	56.6	61.6	-	-	-
VRS-HQ-13B [8]	63.3	61.1	65.5	56.8	54.1	59.4	60.0	57.6	62.5	-	-	-
<i>Latest models via GRPO training</i>												
Omni-R1-8B [34]	61.6	-	-	50.7	-	-	56.2	-	-	-	-	-
Veason-R1-3B [7]	63.0	60.3	65.6	56.8	53.6	60.0	59.9	56.9	62.8	55.2	51.8	58.5
Ours-3B	64.3 (+1.0)	61.6	66.9	58.2 (+1.4)	54.9	61.6	61.2 (+1.2)	58.2	64.3	58.2 (+3.0)	54.6	61.8
Ours-7B	65.9 (+2.6)	63.2	68.7	59.7 (+2.9)	56.6	62.8	62.8 (+2.8)	59.9	65.7	59.4 (+4.2)	56.0	62.8

Table 9: **Performance comparison on RVOS datasets.** The best and second-best results are shown in **red** and **blue** color.

Method	MLLM	DAVIS17			Ref-YouTube-VOS			MeViS		
		$\mathcal{J}\&\mathcal{F}$	\mathcal{J}	\mathcal{F}	$\mathcal{J}\&\mathcal{F}$	\mathcal{J}	\mathcal{F}	$\mathcal{J}\&\mathcal{F}$	\mathcal{J}	\mathcal{F}
Track-GPT-7B [35]	LLaVA-7B	63.2	59.4	67.0	56.4	55.3	57.4	40.1	37.6	42.6
Track-GPT-13B [35]	LLaVA-13B	66.5	62.7	70.4	59.5	58.1	60.8	41.2	39.2	43.1
VISA-7B [30]	Chat-UniVi-7B	69.4	66.3	72.5	61.5	59.8	63.2	43.5	40.7	46.3
VISA-13B [30]	Chat-UniVi-13B	70.4	67.0	73.8	63.0	61.4	64.7	44.5	41.8	47.1
VideoLISA-3.8B [3]	LLaVA-Phi-3-V	68.8	59.4	64.9	63.7	61.7	65.7	44.4	41.3	47.6
GLUS-7B [13]	LLaVA-7B	-	-	-	67.3	65.5	69.0	51.3	48.5	54.2
VRS-HQ-13B [8]	Chat-UniVi-13B	74.4	71.0	77.9	71.0	69.0	73.1	50.9	48.0	53.7
Veason-R1-3B [7]	Qwen2.5-VL-3B	-	-	-	-	-	-	51.2	48.2	54.2
Ours-3B	Qwen2.5-VL-3B	76.1 (+1.7)	72.2	80.0	72.5 (+1.5)	70.5	74.6	53.7 (+2.4)	50.7	56.7
Ours-7B	Qwen2.5-VL-7B	78.6 (+4.2)	75.0	82.2	73.3 (+2.3)	71.5	75.1	54.8 (+3.5)	51.9	57.7

shown in Table 10, this sampling strategy substantially reduces the extra computational overhead from 81% to 40% while maintaining highly competitive performance.

Table 10: Performance and computational overhead comparison of different AKS strategies.

Method	Extra Time	Ref-YT-VOS	ReasonVOS	ReVOS	MeViS
Ours (Full Video)	81%	72.5	58.2	61.2	53.7
Ours (Sample 16 after Full Video)	40%	72.4	57.8	60.9	54.2

Furthermore, we report the average inference time per video in Table 11, split into keyframe selection and segmentation. This breakdown shows that the main runtime bottleneck in VRS remains the segmentation stage (MLLM + SAM2), not keyframe selection. In particular, AKS adds only a small overhead relative to VRS-HQ (12s vs. 11s), while our downstream segmentation stage is actually faster than both prior methods. Thus, the agentic design does not make the overall pipeline disproportionately heavy.

We also conduct a direct efficiency comparison with our concurrent work Veason-R1 in Table 12. Our evaluation reveals that Veason-R1-3B takes a total of 36 seconds per video. This latency occurs because its architecture requires feeding multiple high-resolution frames simultaneously into the MLLM. Due to severe memory constraints, it can only support a maximum of 8 sampled frames as input on a 48GB L20 GPU.

D Intermediate-level evaluations

Keyframe quality and re-selection efficiency. To measure keyframe quality, we compute the ratio between the target object’s pixel area in the selected frame and its maximum area over the full video. As shown in Table 13, AKS consistently replaces suboptimal initial frames with more informative ones, substantially increasing target visibility, while requiring only 1.3–2.4 rounds on average.

Table 11: Inference time analysis.

Method	Keyframe Selection Time	Segmentation Time
VISA	21s	24s
VRS-HQ	11s	28s
Ours	12s (AKS)	19s

Table 12: Inference time comparison with Veason-R1.

Method	Keyframe Selection and Segmentation Time
Veason-R1-3B (Sample 8 frames)	36s
Ours	31s

Intermediate grounding accuracy. To evaluate spatial precision before SAM2 propagation, we compute the Avg IoU between predicted intermediate boxes and ground-truth boxes (converted from masks). The IoU values in Table 14 show that the KTG stage already provides accurate localization before mask propagation.

Necessity of Explicit CoT. To directly evaluate the role of explicit CoT traces, we train an Answer-Only baseline by removing the `<think> ... </think>` content from the training targets and asking the model to predict only the final answer. The SAM2 interface, output format, and all other training settings are kept unchanged, so the comparison isolates the effect of explicit reasoning supervision.

As shown in Table 15, the gains are consistent across all benchmarks, showing that explicit CoT supervision provides a clear benefit beyond predicting the final answer alone. The improvements are especially larger on ReasonVOS (+3.1) and ReVOS (+2.9), suggesting that explicit reasoning helps build a stronger intermediate representation for keyframe verification and target grounding, rather than serving as a simple formatting choice.

E Training curves analysis

We visualize the GRPO training dynamics of the proposed RCoT-Seg in Figures 11 and 12, as well as the CoT-SFT training loss in Figure 13.

We monitor three key metrics during GRPO training: task-aligned reward \mathcal{R} , response length, and the value of KL loss. As shown in Figures 11a and 12a, the model initialized via CoT-based supervision starts with a reward score around 2.1 in AKS task and 4.3 in KTG task, indicating a reasonable ability to generate structured outputs for both tasks. The consistent upward trend in reward reflects effective policy refinement and better alignment with the designed reward function. As can be

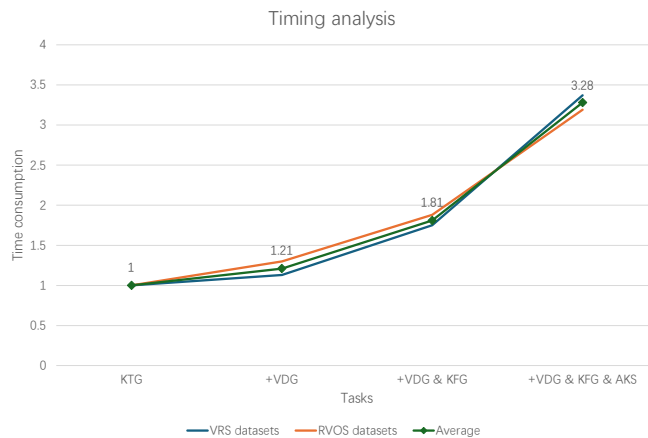


Figure 10: Curves of timing analysis on VRS and RVOS datasets.

Table 13: Keyframe quality and re-selection efficiency.

Metric	Setting	Davis	Ref-Youtube-VOS	ReasonVOS	ReVOS
Area Ratio (%)	Initial	43.0	51.6	37.3	61.0
	Reselected	65.9 (+22.9)	64.1 (+12.5)	58.0 (+20.7)	67.9 (+6.9)
Average Rounds	-	1.4	1.3	2.3	2.4

Table 14: Intermediate grounding accuracy.

Metric	Davis	Ref-Youtube-VOS	ReasonVOS	ReVOS
Avg IoU (%)	75.0	70.4	57.7	60.2

Table 15: Necessity of Explicit CoT.

Method	Davis	Ref-Youtube-VOS	ReasonVOS	ReVOS
Answer-Only	73.9	69.8	55.1	58.3
Explicit-CoT (Ours)	76.1(+2.2)	72.5(+2.7)	58.2(+3.1)	61.2(+2.9)

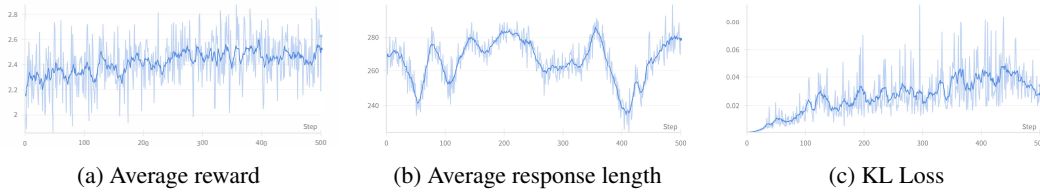


Figure 11: Curves of GRPO training for AKS task.

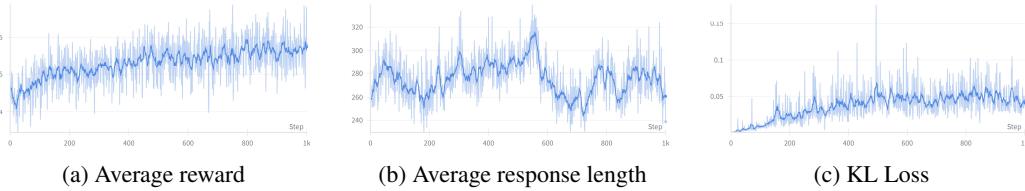


Figure 12: Curves of GRPO training for KTG task.

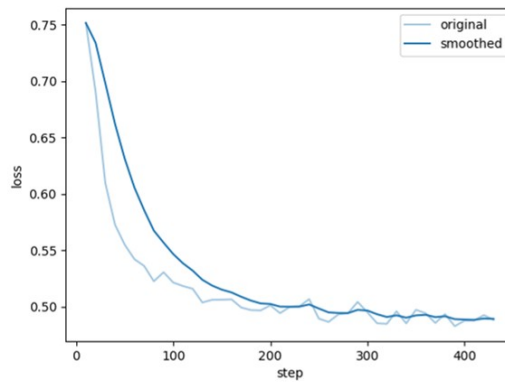


Figure 13: Curve of CoT-SFT training loss.

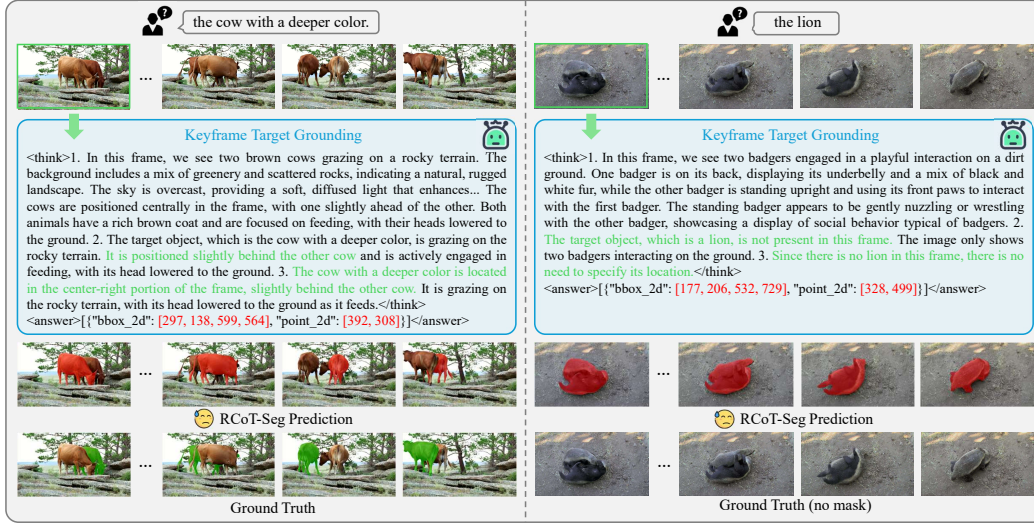


Figure 14: Visualization of failure cases on the ReVOS dataset. RCoT-Seg reveals inconsistencies between its reasoning traces and final segmentation outputs, and demonstrates limited adaptability in the zero-target task.

seen from Figures 11b and 12b, the average response length of our model for both tasks remains stable at around 300 tokens. As depicted in Figures 11c and 12c, the KL divergence progressively increases as the model shifts away from the initial policy to explore more reward-driven behaviors. It eventually plateaus, signifying convergence toward a consistent and reward-aligned policy under the regularization constraint.

The CoT-SFT training loss of the model shown in Figure 13 demonstrates a consistent and significant decrease from approximately 0.75 to around 0.48 over 400 steps, indicating effective learning convergence.

F Limitations

In this study, the construction of the segmentation dataset does not incorporate samples for zero-target segmentation [27], which limits the model from to handle zero-target segmentation tasks. When the instruction refers to an object absent from the video, the model consequently produces incorrect segmentation results, which could be mitigated by developing a more comprehensive dataset and modifying the corresponding evaluation strategy. Furthermore, regarding dataset construction, unlike some existing methods that rely on massive frontier models for data synthesis, our approach utilizes the relatively smaller open-weight Qwen2.5-VL series. Specifically, we employ Qwen2.5-VL-7B to construct the Chain-of-Thought reasoning traces and Qwen2.5-VL-3B to generate the video descriptions.

G Failure case analysis

Figure 14 presents some failure cases of RCoT-Seg on the ReVOS [30] dataset. In the left example, the model generates a correct reasoning trace, accurately identifying the cow with a deeper color and describing its relation to another cow. However, the predicted masks fail to align with the described target, revealing an inconsistency between the reasoning trace and the final segmentation outputs. In the right case, it is a zero-target scenario where the lion is not present in the video sequence. The model correctly identifies this situation in its reasoning trace, and yet it still outputs incorrect localization information, demonstrating its limited adaptability in the zero-target task. Figure 15 further reveals the misjudgment of RCoT-Seg when performing the AKS task. In this case, the target object has not yet appeared in the keyframe deemed correct by the model, resulting in an incorrect segmentation.

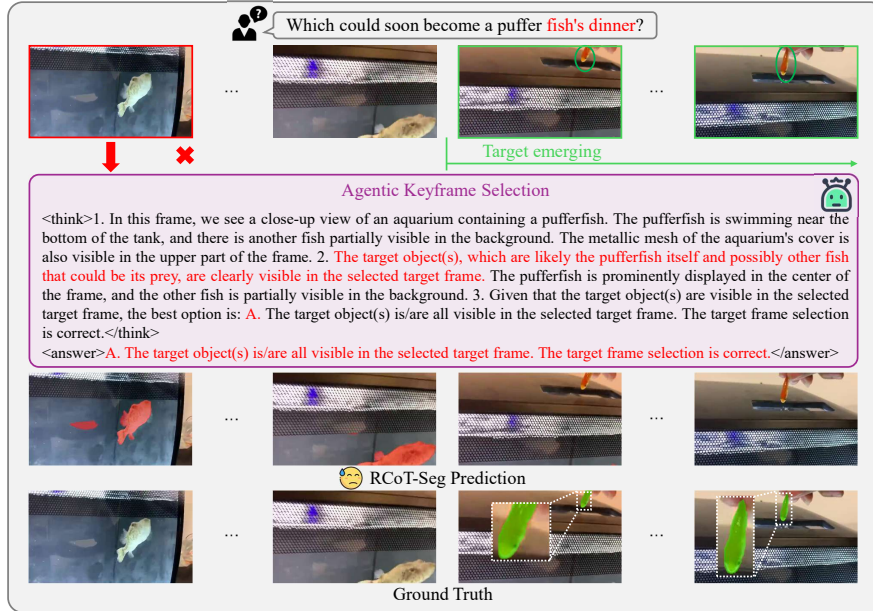


Figure 15: Visualization of failure cases on the ReVOS dataset. In this case, RCoT-Seg erroneously classifies an invalid keyframe as valid in the AKS task.

H More qualitative comparison

We present additional visual comparisons of RCoT-Seg-3B with GLUS-7B [13] on the ReasonVOS [3] dataset and VRS-HQ-7B on the ReVOS [30] dataset, to underscore its robust reasoning capabilities and enhanced fine-grained grounding performance.

The qualitative comparison of RCoT-Seg-3B with GLUS-7B is shown in Figure 16. In the left example, various pedestrians, vehicles, and traffic facilities at the intersection constitute a complex video scene. GLUS-7B produces an incorrect segmentation result. In contrast, the proposed RCoT-Seg-3B first accurately identifies the incorrectly selected keyframe through the AKS task and reselects the correct keyframe. Then, in the KTG task, the model correctly identifies the target object (who is not wearing a bright yellow jacket) based on the provided video description and accurately predicts the segmentation masks. In the right case, the query involves action logic (unmoving, with its head swinging back and forth), which requires the model to perform reasoning. RCoT-Seg-3B accurately identifies the correct target object (the larger cow in the foreground) in the reasoning trace and provides an accurate masks prediction, whereas GLUS-7B produces an incorrect answer.

Figure 17 visualizes the segmentation maps of RCoT-Seg-3B, GLUS-7B [13] and VRS-HQ-7B [8] on the ReVOS dataset. In the left example, RCoT-Seg-3B correctly segments the bird in the upper right corner of the scene, whereas both VRS-HQ-7B and GLUS-7B confuse this bird with another incorrect target object due to their overlap. In the right case, RCoT-Seg-3B accurately segments the target object (transparent, made of plastic), whereas both GLUS-7B and VRS-HQ-7B confuse it with other objects, demonstrating our model's superior ability to comprehend object materials and colors.

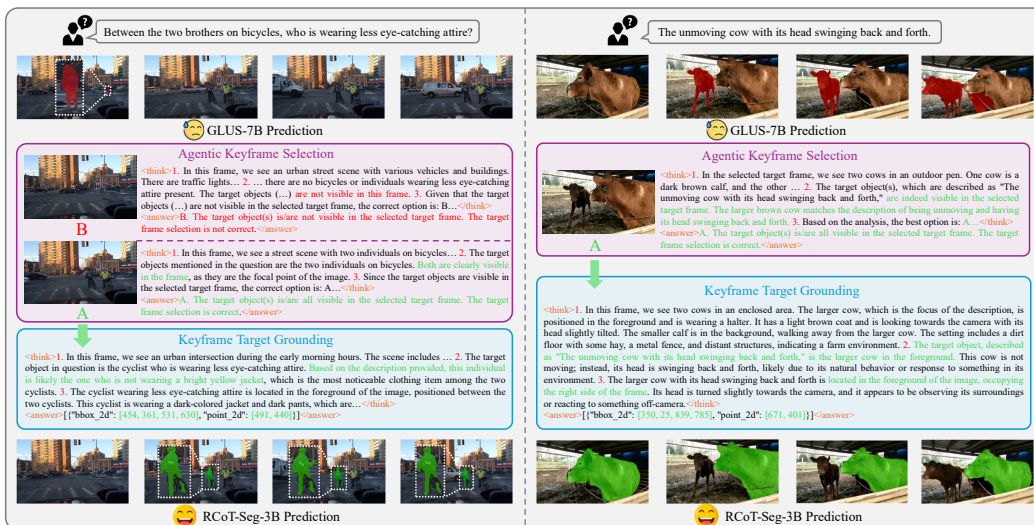


Figure 16: More qualitative comparison on the ReasonVOS dataset.

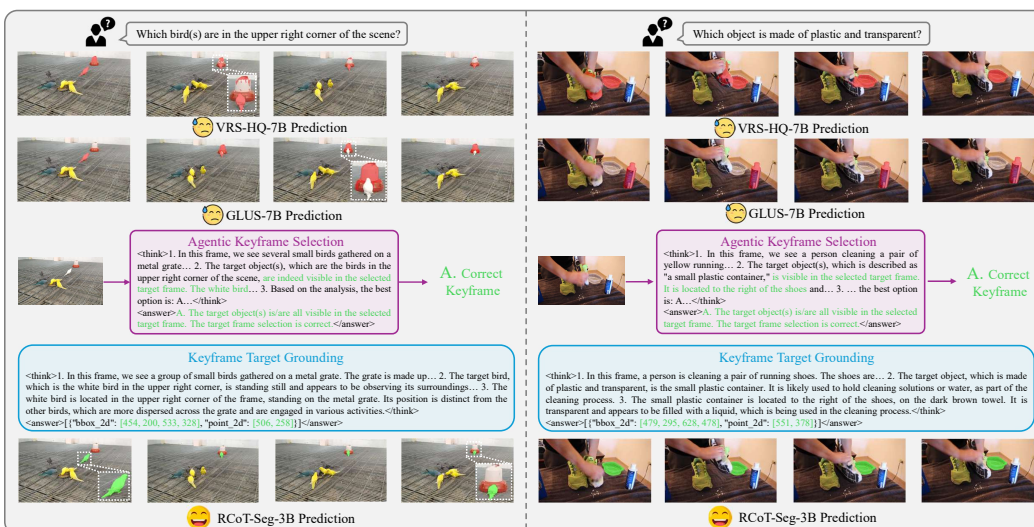


Figure 17: More qualitative comparison on the ReVOS dataset.